

# Greatest Prime Factor

Linus Vepstas

December 2018 formalization of April 2016 web version

## Abstract

There appears to be very little written about the greatest prime factor (gpf) function, and especially its generating functions. This paper provides a numerical, visual survey of its exponential generating function, illustrating its remarkable symmetry properties.

## Introduction

A cursory search of the Internet indicates that very little is known[1] about the greatest prime factor function  $\text{gpf}(n)$  that returns the largest prime divisor of  $n$ . Some values and additional references are given in the OEIS A006530[2]. I was unable to find anything at all discussing the typical analytic formulations of this sequence, such as the ordinary generating function

$$G(z) = \sum_{n=1}^{\infty} \text{gpf}(n) z^n$$

or the exponential generating function

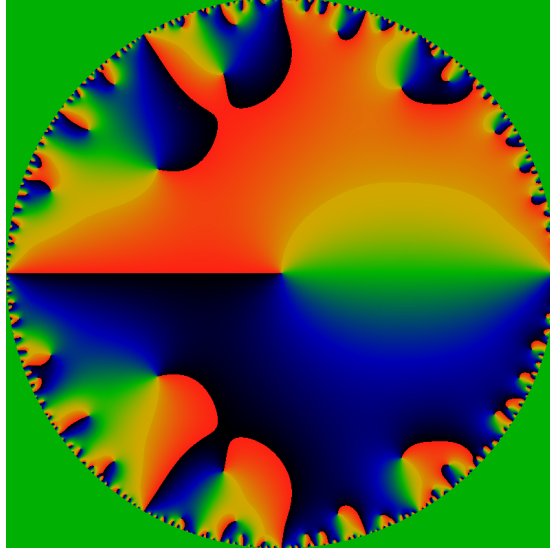
$$E(z) = \sum_{n=1}^{\infty} \text{gpf}(n) \frac{z^n}{n!}$$

Thus, I thought I would do a bit of numerical exploration. The exponential generating function exhibits a variety of remarkable symmetric and fractal properties. On the one hand, this is perhaps not surprising, as fractal symmetries are common in number theory.[3, 4] On the other hand, the actual figures make it clear that this function is quite unlike anything else. This paper is a numerical and visual exploration of the exponential generating function, exposing its patterns of self-similarities. It offers essentially no analytic results; despite the “obvious” structure, obtaining exact results appears to be difficult.<sup>1</sup>

---

<sup>1</sup>Some of the figures in this text show richer detail, and are particularly striking when they are magnified. Due to space limitations, they are kept rather small in this text. Larger images can be found at <https://linas.org/art-gallery/gpf/gpf.html>

Figure 1: Phase of the Ordinary Generating Function



This figure shows the phase (arctan) of the function  $G(z)$ ; that is, it shows  $\varphi(z)$  where  $\exp i\varphi(z) = G(z)/|G(z)|$ . The color coding is such that red indicates a phase of  $+\pi$ , green is a phase of zero, and black is a phase of  $-\pi$ . The sharp red-black transitions are where the phase wraps around by  $2\pi$ . These transition lines can only terminate on zeros and on poles; which is which can be identified by whether the phase wraps counterclockwise or clockwise. Here, the lines that terminate inside the unit circle all terminate on zeros; the edge of the circle is ringed with both poles and zeros. The exterior of the unit circle is colored green: there is no analytic extension of  $G(z)$  outside of the unit circle.

## Phase Plots

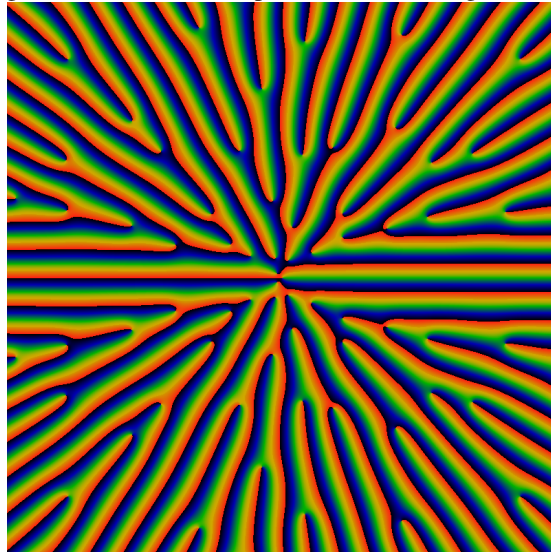
Figure 1 is a phase plot of the ordinary generating function  $G(z)$  for complex  $z$ . This function has a radius of convergence of one, with what appears to be essential singularities scattered all about the unit circle. The function is not obviously any kind of modular form, but is suggestive of some sort of theta function. That is, there is some vague fractal self-similarity-ish behavior, which is very typical of any sort of modular form or function;[5] however, its not in any "obvious" form that *e.g.* the  $j$ -function or the Eisenstein functions would have. On the other hand, it seems that just about any "random" sequence has a similar general appearance, and so there is not much intuitive information that can be extracted from this figure.

Figure 2 shows the a phase plot of the exponential generating function  $E(z)$  on the complex  $z$  plane. This function appears to be entire! The width of the figure is 120; that is, it graphs the domain  $-60 \leq x, y \leq +60$  for  $z = x + iy$ . The rays all appear to terminate on zeros of the function; there do not appear to be any poles anywhere

(except at infinity, of course). But then, the absence of poles should be clear, as  $\text{gpf}$  is bounded:  $\text{gpf}(n) \leq n$  and so one would expect  $E(z)$  to be bounded by  $e^z$ .

The red-black color transition in both figures 1 and 2 indicates a location where the phase changes by  $2\pi$ . Such color transition lines can only ever terminate on poles and zeros. Since phases can only wrap counterclockwise around a zero, and clockwise around a pole, such transition lines can never connect two zeros; they can only connect a zero to a pole. Since  $E(z)$  has only zeros on the (finite) complex plane, the transition lines seen in figure 2 must necessarily extend, more-or-less radially, out to infinity, where they meet an essential singularity. This simple effect explains most of the visual structure of this image.

Figure 2: Phase of the Exponential Generating Function

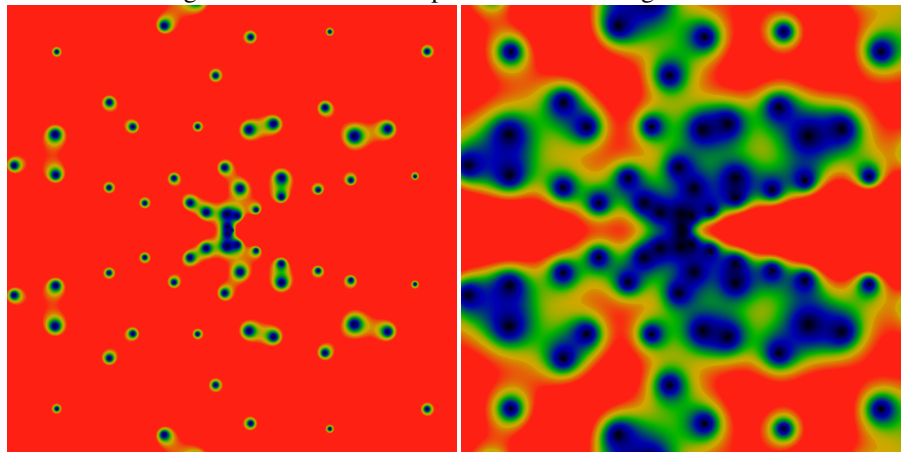


This figure shows the phase plot of  $E(z)$  on the complex  $z$  plane. The color scheme and its interpretation is the same as in Figure 1. The width of the figure is 120; that is, it graphs the domain  $-60 \leq x, y \leq +60$  for  $z = x + iy$ . It is convenient to define  $\text{gpf}(0) = 0$  and  $\text{gpf}(1) = 1$ , so that the zero at  $z = 0$  is a simple zero.

The regularity of the thickness of these phase-fingers immediately provides a hypothesis about the zeros. The figure reveals that the zeros seem to be more or less uniformly distributed about the complex plane. In order for the fingers to remain of uniform width, this implies that the number of zeros within a circle of radius  $r = |z|$  must be proportional to the circumference of the circle. Were this not the case, the fingers could not stay at a quasi-uniform width. Thus, visual evidence applied to Cauchy's argument principle suggests that

$$N(r) = \frac{1}{2\pi i} \oint_{|z|=r} \frac{E'(z)}{E(z)} dz = \mathcal{O}(r)$$

Figure 3: Zeros of the Exponential Generating Function



Both figures show the same domain as in figure 2; that is, are bounded as  $-60 \leq x, y \leq +60$  for  $z = x + iy$ . Both figures show the magnitude  $|E(z)|e^{-|z|}$ , but with different color scales. On the left, the color map is such that red corresponds to values of 1.0 or greater, and green to values around 0.5. On the right is exactly the same image, but the color map scaled by 0.24. That is, red corresponds to values of  $4.17 \approx 1/0.24$  or greater, and green to values of about 2. The color scheme on the right exposes a clustering of the zeros that is less evident on the left.

where  $N(r)$  is the number of zeros of  $E(z)$  within a circle of radius  $r = |z|$ . This is explored in greater detail in a later section, where the numerical evidence suggests that

$$N(r) = r + \mathcal{O}(\log r)$$

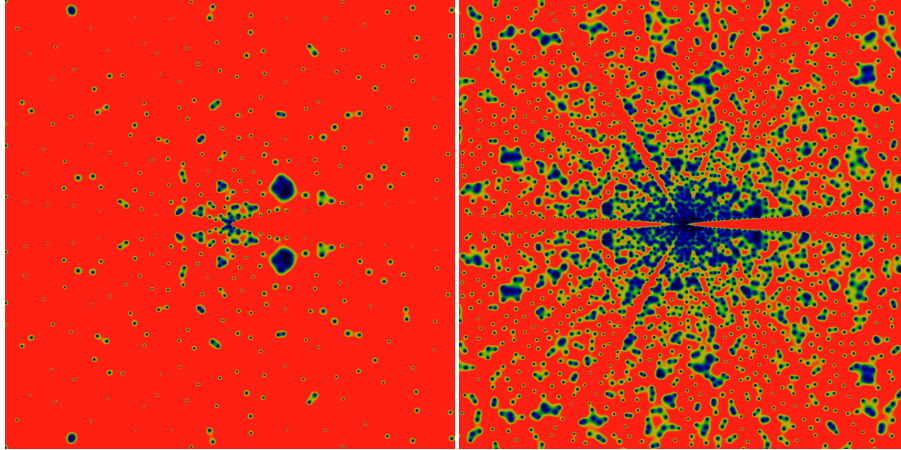
as  $r \rightarrow \infty$  (or, at least, for values of  $r$  that are several orders of magnitude larger).

## Zeros

Figure 2 suggests that the zeros are fairly uniformly distributed; however it is fairly cluttered, so it's hard to tell quite where they really are. If there is regularity, it is obscured. Thus, figure 3 is used to explicitly expose the location of zeros as black dots in the image. The figure shows the absolute value  $|E(z)|$ . Observe that  $E(z)$  diverges as  $e^{|z|}$  for large  $z$ ; thus the color scale is selected to show  $E(z)e^{-|z|}$  to make the zeros more easily visible.

The zeros in figure 3 cluster in a suggestive way. Perhaps one should zoom out. This is shown in figure 4. This exposes a new and interesting feature: rays! Lanes that are free of any zeros! Rays for the cyclic groups  $\mathbb{Z}_2$  and  $\mathbb{Z}_3$  are clearly visible, and with some peering, the rays for  $\mathbb{Z}_5$  can be seen as well. There's a hint of  $\mathbb{Z}_7$ . Notably absent (or just hard to see?) are rays for  $\mathbb{Z}_4$ . This seems to lead to a natural conjecture that zeros only occur on rays for  $\mathbb{Z}_p$  for  $p$  prime.

Figure 4: Zoom-out of the EGF



Both figures show the magnitude  $|E(z)|e^{-|z|}$ ; the one on the left is for  $-360 \leq x, y \leq +360$  while the one on the right is for  $-2160 \leq x, y \leq +2160$ . The big blue-black blobs in the left image are five different zeros, fairly close to each other. The color scale of the left image is adjusted so that green is about 0.2, and red is any value of 0.4 or greater. The color scale of the right image is again adjusted so as to make the large  $|z|$  zeros more clearly visible. In this case, values greater than 0.031 are red.

The above conjecture can be explored by taking slices along rays, shown in the figure 5. It shows six slices, taken along the direction  $z = e^{i\theta}$  for  $\theta = 0, \pi, 2\pi/3, 2\pi/4, 2\pi/5, 2\pi/6$ . The leading divergence of  $e^{|z|}$  has been removed, leaving a divergence that seems to be about of order  $|z| / \log |z|$ . Notable in this graph is that no zeros are visible along the rays for  $\theta = 2\pi/4$  and  $\theta = 2\pi/6$ . This suggests the the above conjecture about rays at primes vs. composites was incorrect.

Most notable about this picture is the pronounced smooth oscillations along each ray. It's visually clear that the wavelengths get longer as  $|z|$  gets larger. Closer examination shows that the wavelength goes as the square-root of  $|z|$ .

A similar exploration of rays directed along quadratic irrationals suggests that such rays pass very close to zeros on a number of occasions, but none actually pass through a zero. Figure 6 shows a phase plot of one such ray, graphing the real vs. the imaginary part of  $E(z)$  for  $z$  running from 0 to 1000. The close passes are visible: keep in mind that since the leading exponential scaling is removed, the close passes visualized here are indeed very close. At any rate, the phase along a slice is not simple or regular; the figure is a mess.

So where are the zeros located? Hard to say. The exploration of other angles, including simple fractions (without any factors of  $\pi$ ) suggests that these, too, manage to not hit any zeros, at least, not for  $|z| < 1000$ , although the ray for  $\theta = 1/3$  really sure does come very, very close.

Below is a table of the 11 zeros nearest the origin. The coding is such that  $z =$

Figure 5: Slices along Rays

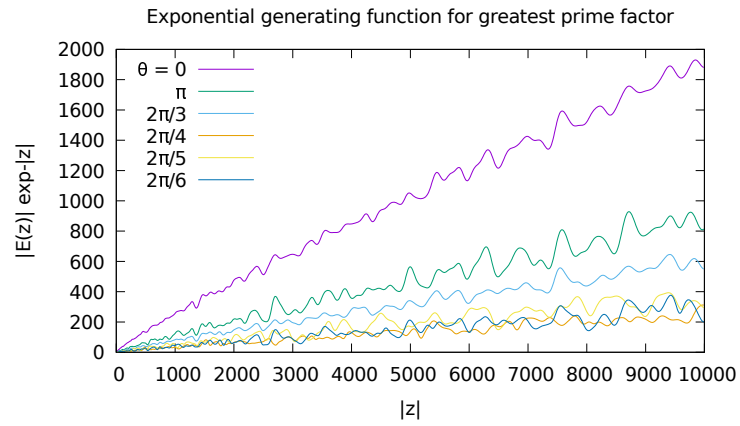
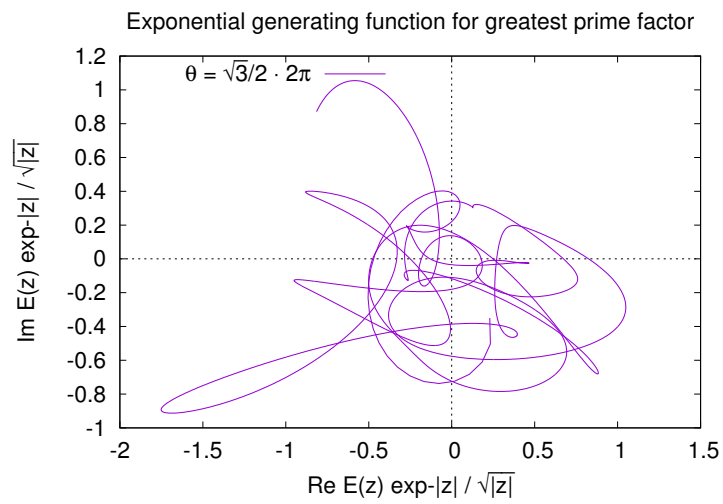


Figure 6: Slice along a quadratic irrational



$re^{i\pi\varphi} = x + iy$ . Accuracy is good to about the last digit. Plouffe's inverter[6] doesn't seem to know any of these numbers. They're presumably all some unknown transcendentals.

$r$	$\varphi$	$x$	$y$
1.5307945356883	0.78184092190433	-1.1851209706937	0.9689273426400
4.0367224459103	0.39186518257935	1.3451122542394	3.8060216931609
4.5623453697754	0.60435053770449	-1.4690131787199	4.3193744401079
8.3702116601813	0.22324068364269	6.3947066808728	5.4007564008976
8.4224011490127	0.80891465405978	-6.9498220138446	4.7578162102767
11.344004468582	0.44048322811112	2.1087356654558	11.146285088604
13.460094569784	0.81744853194064	-11.306557973367	7.3031426538461
15.804853981417	0.18788938300147	13.130504695764	8.7967753073744
16.909948423814	0.53886030109517	-2.0592969204905	16.784089248133
19.238778607721	0.26037809273961	13.153182482454	14.040099461904
20.867068162569	0.76767832172763	-15.551551998824	13.913438256922

Below is another table of zeros, this one for  $EG(\text{ngpf}; z)$ , where  $\text{ngpf}(n) = n \cdot \text{gpf}(n)$  and

$$EG(f; z) = \sum_{n=0}^{\infty} f(n) \frac{z^n}{n!}$$

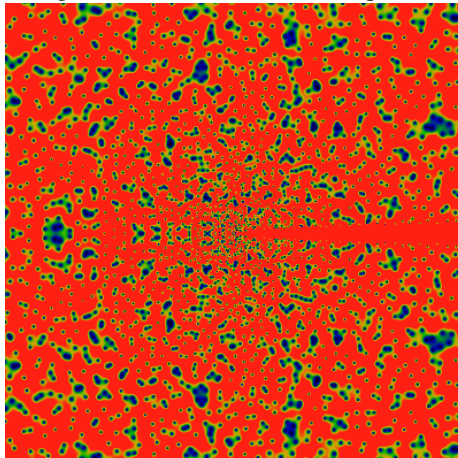
That is, this is the same gpf exponential series, except that it's been shifted over by one. That is,

$$EG(\text{ngpf}; z) = z \frac{d}{dz} E(z) = \sum_{n=1}^{\infty} \text{gpf}(n) \frac{z^n}{(n-1)!}$$

Note that these are in the same general location as the above, except that they have moved inwards a bit.

$r$	$\varphi$	$x$	$y$
0.8802234956260	0.83295289206477	-0.7617693460645	0.4410225228358
3.2375048946125	0.42458721923649	0.7598622312185	3.1470696420968
3.7441361185659	0.59817818048564	-1.136602428757	3.5674486952574
7.4736771339129	0.23110162504623	5.5889493606786	4.9618035980621
7.5113122974420	0.80582634942347	-6.1565697810839	4.3030757558226
10.41426766772	0.44047959714246	1.9360237252942	10.232730974183
12.602613307375	0.81645934805374	-10.564968103744	6.8707576832617
14.800600506967	0.19203401986558	12.187879585189	8.397223742630
15.997814072863	0.53774902696863	-1.8927698515501	15.885448605531
18.340908478517	0.25911033247266	12.592535370681	13.334803213977
19.957065054996	0.7682384241160	-14.896747647415	13.280487759815

Figure 7: Uniform Random Sequence



The exponential generating function  $EG(rs; z)$  for a random, uniformly distributed sequence  $2 \leq rs(n) \leq n$ . Note the absence of rays, except for one along the positive  $x$ -axis. This can be accounted for by the fact that none of the  $rs(n)$  are zero (or negative), and thus cannot factor in such a way that there would be a zero on the positive  $x$ -axis. This is an expression of Descartes's rule of signs, expanded from polynomials to series.

The image runs out to a radius of 2160; to get the color map correct, the leading exponential divergence is removed, as is also a factor of  $\log^2(r)/r$ . In other words,  $rs(n)$  does have a different asymptotic behavior than  $gpf(n)$ .

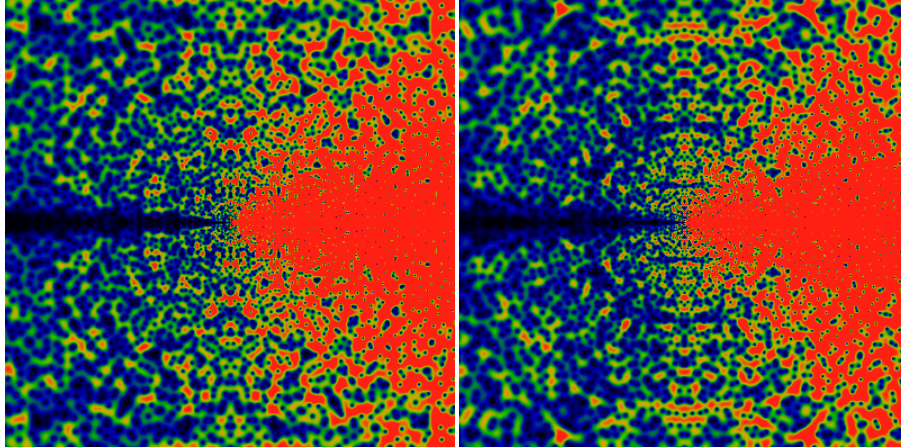
---

## Random Sequences

Before one gets too excited, it's worth asking: how much of the general shape of this function is due to the fact that the greatest-prime-factor sequence is being used, and how much is "generic", shared by any similar series? To answer this question, one can generate random series  $rs(n)$  that roughly resemble  $gpf(n)$ . Consider, first, the series having the property that  $2 \leq rs(n) \leq n$ , but otherwise having a uniform distribution in this range. In such a case, one finds that  $EG(rs; z)$  does have zeros scattered all over the complex plane, in a roughly similar distribution; however, the rays are completely absent, as can be seen in figure 7.

Perhaps the rays are due to the primes? One can consider a random distribution  $rps(n)$  having the property that  $2 \leq rps(n) \leq n$  and also that  $rps(n)$  is prime. Figure 8 shows  $EG(rps; z)$  for two such random uniformly distributed sequences. No rays, but hints of rings! Curious! And also, an odd left-right symmetry! Clearly, more work can be done in this general area.

Figure 8: Random Prime Sequences



The exponential generating function  $\text{EG}(\text{rps}; z)$  for a random, uniformly distributed sequence of primes, with  $2 \leq \text{rps}(n) \leq n$ . Such images all show suggestions of zero-free rings!

## Zero-free Lanes

The singular ray visible in figure 7 provides a key for how one might want to hypothesize and talk about the zero-free lanes. When a sequence  $f(n)$  has the property that  $0 < f(n)$  for all  $n$ , then the exponential generating function  $\text{EG}(f; z)$  cannot have any zeros along the positive real axis. That is, it is impossible to find a factor  $(z - b)$  for real, positive  $b$ . Without a negative  $f(n)$ , there is nothing to introduce the needed minus sign. With this in mind, the rotated function

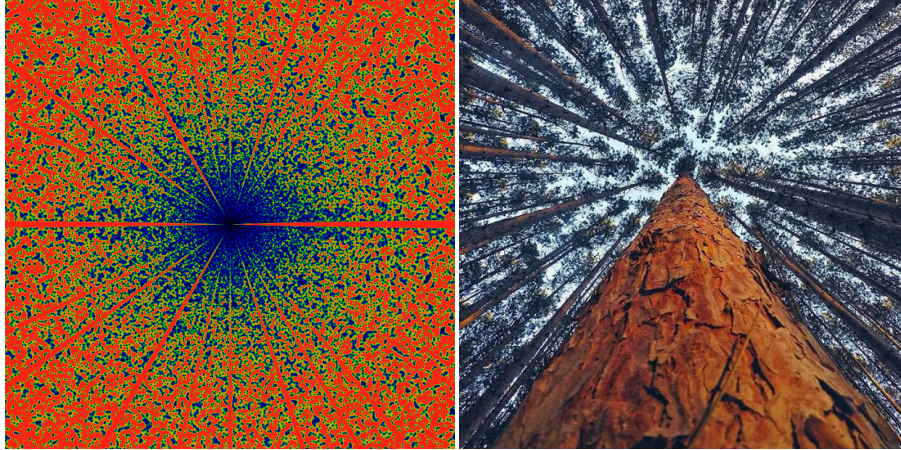
$$E_{p/q}(z) = \sum_{n=1}^{\infty} \text{gpf}(n) e^{-2\pi i p n/q} \frac{z^n}{n!}$$

which apparently has no roots on the real axis, whenever  $p/q$  is a rational.

Continued zooms are striking. Figure 9 shows a further outward zoom. This time, a ray at  $\mathbb{Z}_4$  is incontrovertibly visible. The width of the rays, relative to their angular distribution, does not follow any obvious pattern explainable by hand-waving. The blueness in the center, *vs.* the redness towards the edges, is annoying. This suggests that the asymptotic behavior has been misjudged. This is handled next.

What are the angular locations of the zero-free lanes? These are shown in figure 10, and are labeled with Farey fractions, to show their positions, and with a bunch of Ley lines, to demonstrate their heights. The graph was obtained by computing the absolute value  $|\text{EG}(\text{gpf}; z)|$  along radial slices. Plotting just one radial slice is noisy and indistinct, contradicting what is visually obvious. Thus, some noise cancellation is in order. This can be done by averaging together multiple radial slices; the figure below shows an average of 500 of them, taken near the radius  $r = |z|$  of about 16000. The

Figure 9: Hints of Projective Geometry



The left image shows  $E(z)$  for  $-20000 \leq x, y \leq +20000$ . The right image is from a photo of trees, posted by [Mian Faisal on Google+](#). The visual resemblance suggests that there must be some way of understanding  $E(z)$  in terms of projective geometry, possibly starting from ascending vertical pegs planted on a square grid (e.g. and then deriving properties from the symmetries of a square grid: viz. the modular group  $SL(2, \mathbb{Z})$  which already has rampant connections to analytic number theory.) A more precise hypothesis is elusive.

---

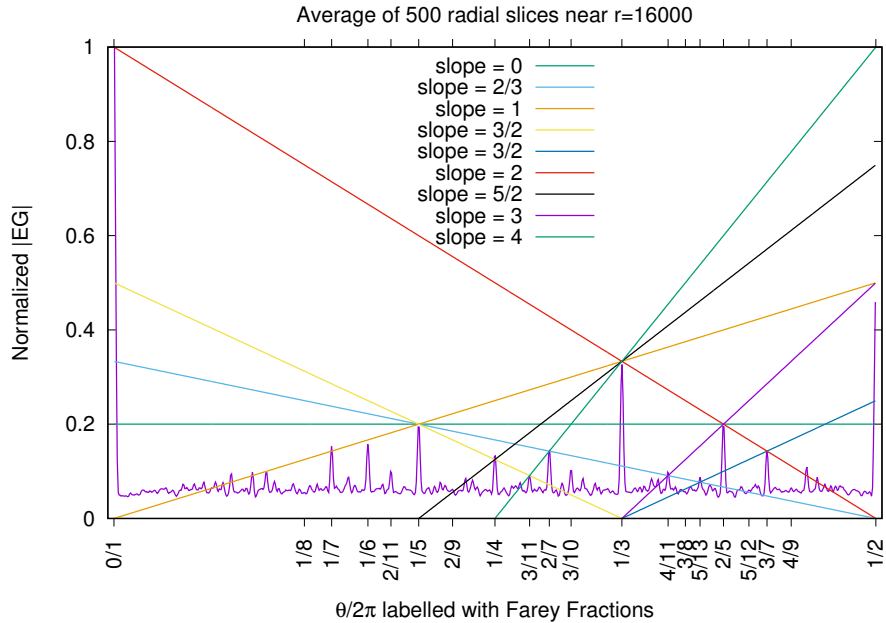
zero-free lanes are the spikes. The tallest spike, at the angle of zero, was normalized to unit height; it sets the overall scale.

The spikes clearly correspond to the Farey fractions. A few seem to be missing: for example,  $2/9$  and  $1/8$  seem to be missing. Before jumping to conclusions, though, it might be the case that these are drowned in the noise. The heights of the spikes are very clearly predicted by straight lines with rational slopes, and are in Farey-order. The tallest spike is at  $0/1$ , and by symmetry, also at  $1/1$ . The first Farey fraction between these two is  $(0+1)/(1+1)=1/2$ , which is the second-tallest spike. Between these two is the next Farey fraction; it lies between  $0/1$  and  $1/2$  and so is  $(0+1)/(1+2) = 1/3$  – which is the location of the next tallest spike. After that, there are two Farey fractions:  $(0+1)/(1+3)=1/4$  and  $(1+1)/(2+3)=2/5$ . Argh! The pattern breaks down! Although the spike at  $2/5$  is indeed the next tallest, the spike at  $1/4$  is unexpectedly short. How is that even possible? Oh well.

Anyway, the two spikes at  $1/5$  and  $2/5$  seem to be of exactly the same height. The next row of the Farey triangle is  $1/5, 2/7, 3/8$  and  $3/7$ . Clearly, there's a tall spike at  $3/7$ , same height as  $2/7$  but taller than  $2/8$  and shorter than  $1/5$ . So something throws off the regular patterning, even though the Ley lines clearly indicate that there is an exceptional amount of regularity.

Note that the heights are absolute heights, and not the heights relative to the noise floor. Presumably, working at more distant radii, and taking more averages would drop

Figure 10: Locations of Zero-free Lanes



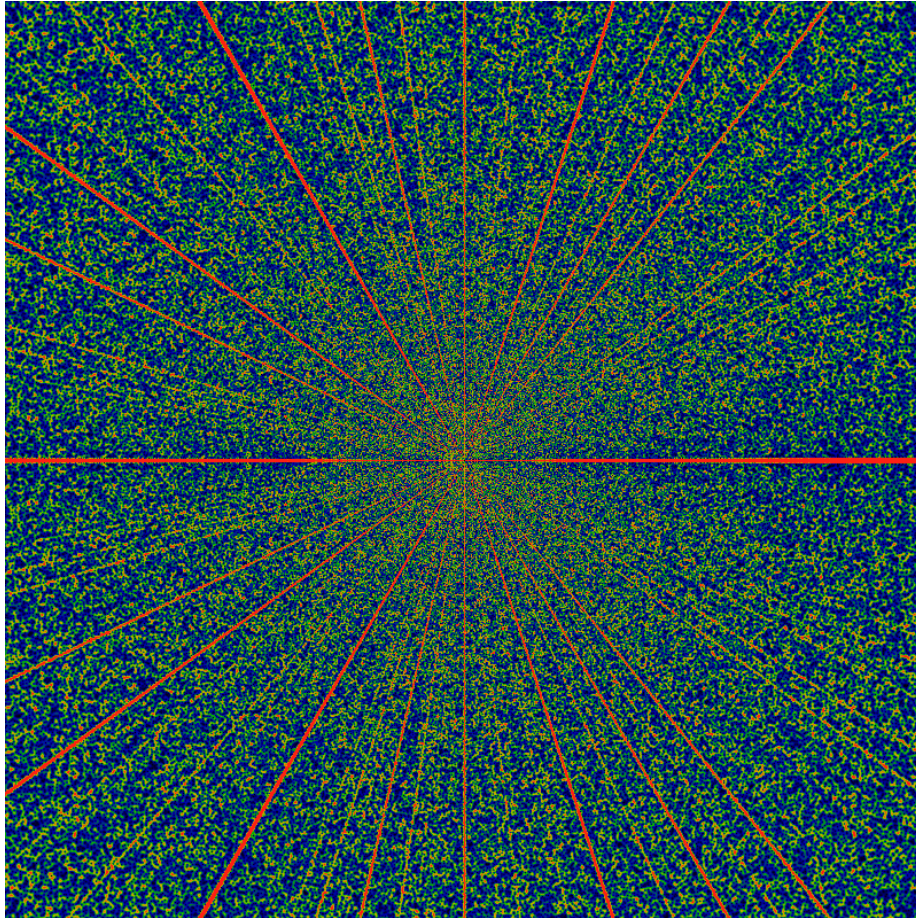
the noise floor; in the limit going to zero, I suppose.

## Asymptotic behavior

Figure 11 shows  $E(z)$  over a wider domain still. It uses a different normalization than the earlier pictures: it multiplies  $E(z)$  by a term  $4r^{-1} \log(r) \exp(-r)$  where  $r = |z|$ . That is, the leading exponential divergence is easily brought under control by the exponential term, leaving a much weaker divergence. Dividing by  $r$  seems to overcompensate; multiplying by the log term seems to be just about right. The factor of 4 is just what is needed to get a pleasing color balance in this picture: again red areas represent values greater than 1, green are the values near 0.5, and blue-black are areas of about 0.2 or less. (No other processing is applied to this image, nor to any other image in this text – the data is always presented in its "raw" form; the colors accurately represent the actual magnitude of the function, as presented).

The most notable aspect of this image, as compared to the earlier ones, is the narrowing of the rays. If one asked for the number of zeros in a pie-sliced wedge, and graphed that as a function of the angle, one would see a devil's-staircase type function. But, as this image shows, the treads on those stairs decrease in size as the radius of the circle increases. The rate is unclear; perhaps it goes as the square-root of the radius? That is, there are lanes that are completely free of zeros; these lanes get wider for larger radius, but at a sub-linear rate. They would have to, to make room for finite-width lanes

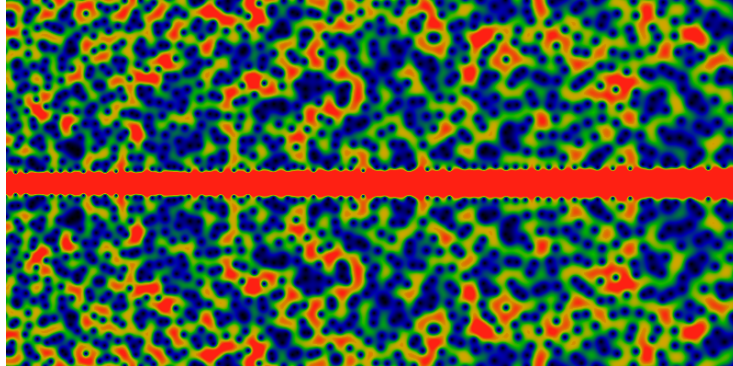
Figure 11: Asymptotic Rays



The function  $4E(z)e^{-|z|}\log|z|/|z|$  for  $-1.25 \times 10^5 \leq x, y \leq +1.25 \times 10^5$ . The color coding is the same as in all other figures.

---

Figure 12: Ray Close-up



How real or illusory is the Moiré patterning? Below shows a close-up, running along the domain  $24000 < x < 48000$  and  $-12000 < y < 12000$ . There is a hint of yet more structure – there seem to be diagonal arrowhead/feather lines. Individual zeros are clearly distinguishable, and it is interesting how they line up so regularly, maintaining a uniform lane.

---

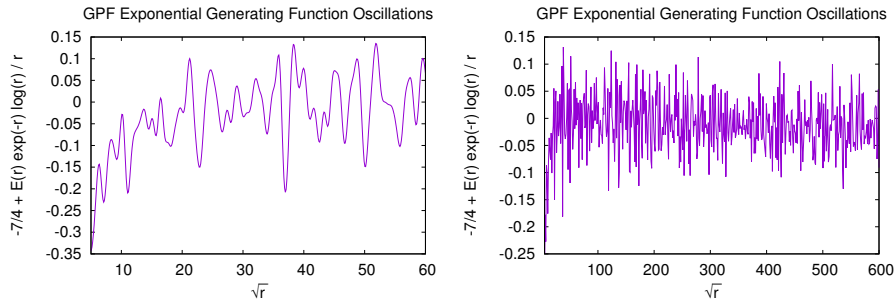
for every rational! A formula for the lane-width is discovered in a later section, below.

The widening of these zero-free lanes is one of the more interesting aspects of this image. Clearly, this image, more strongly than any other, suggests of a ray for every rational. The simplest rationals have the widest lanes; but what, exactly, constitutes "simplest", here? If the rays are arranged according to widths, do they come in Farey-fraction order?

Also notable is a vague hint or suggestion of Moiré patterning along the  $x$ -axis. Recall that Moiré patterns occur when one regular (cyclic) grid pattern is superimposed on another, but shifted over. In this case, one regular pattern are the square pixels of the image; the other is the location of the zeros. The appearance of a Moiré pattern is then strong evidence that the location of the zeros are not "random", but are correlated in some regular, cyclic way (as one moves from ray to ray). But of course it is: figure 5 shows six slices taken along a constant angle (six rays). These each show a characteristic oscillation with some very strong Fourier components. The Moiré patterns are these same Fourier components, interfering with the characteristic pixel size. A closeup of a ray can be seen in figure 12.

The asymptotic behavior of the generating function can be guessed at by numerical means. Figure 13 show the re-scaled quantity  $-7/4 + E(r)r^{-1}e^{-r} \log(r)$  as a function of  $\sqrt{r}$ . Strong periodic oscillations are clearly visible. The rescaling hides just how small these oscillations are: So, for  $\sqrt{r}=60$ , one has  $r = 3600$  and  $re^r / \log r \approx 10^{1566}$  – a truly large number, and so the amplitude of the oscillations is 1566 orders of magnitude smaller than the function itself! Yes, the exponential divergence is obvious. What is have left is then  $r / \log r \approx 440$  so the rescaling pulls out two orders of magnitude. That this does indeed seem to be the correct asymptotic scaling is reinforced by the graph that shows the same oscillations out to  $\sqrt{r} = 600$ . This corresponds to  $r = 3.6 \times 10^5$

Figure 13: Asymptotic Behavior



Oscillatory component remaining, after removal of a large asymptotic factor. Both figures show  $-7/4 + E(r) r^{-1} e^{-r} \log(r)$  along the real axis. Note the vertical scale of these graphs: one concludes that  $E(r)$  is exceedingly smooth, given how small these residual variations are. This is not numerical error; the data is obtained using arbitrary precision codes with sufficient cross-checking to assure that these graphs are accurate, as shown. In particular, the right-hand graph requires well in excess of 1600 decimal places of accuracy to obtain correctly.

and  $r/\log r \approx 2.8 \times 10^4$ , which is still quite large, as compared to the magnitude of the oscillations! That the oscillations are happening around  $7/4 = 1.75$  is just a suggestion from the graph: closer numerical work suggests that the centerline is perhaps at 1.744.

## The Fourier Spectrum

The periodic behavior in figure 13 suggests a question: What's the Fourier spectrum? Low-frequency noise, it seems. Figure 14 shows the amplitude of the Fourier components, as a function of frequency. Specifically, this shows the amplitude  $\sqrt{a^2(\omega) + b^2(\omega)}$  where the Fourier components are

$$a(\omega) = \int f(t^2) \cos(2\pi\omega t) dt$$

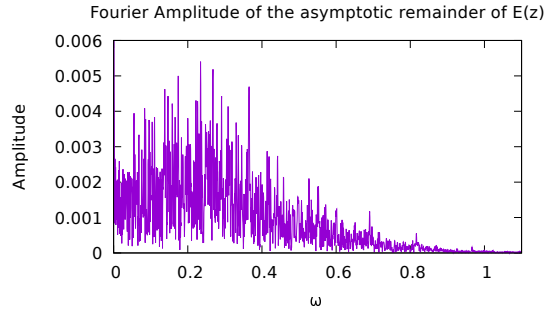
$$b(\omega) = \int f(t^2) \sin(2\pi\omega t) dt$$

and where  $f(r)$  is the asymptotically rescaled generating function:

$$f(r) = -7/4 + E(r) r^{-1} e^{-r} \log(r)$$

The integration is taken over the range  $10 < t < 610$ . This corresponds to the right graph of figure 13. Again, its hard to overemphasize how small these oscillations are: the integral is performed over a region where the generating function blows up by 161 thousand orders of magnitude! Take some caution, however, in interpreting the graph scale: the amplitude at any given frequency is probably either zero or infinite; this

Figure 14: Fourier Spectrum



graph is just an approximation to the true Fourier spectrum, which (I presume) consists of Dirac delta functions of various weights at various irrationals. That is, it seems reasonable to hypothesize that the support for the Fourier spectrum is a Cantor space; a comb that is zero at the rationals, but having integrable support on what remains.

Perhaps the most notable feature of this graph is that, indeed, it looks very noisy: there is no obvious self-similar structure in it. Its hard to make out what the fall-off in frequency is: its perhaps cubic. In case you are wondering: no, this is *NOT* numeric noise; this can be most easily seen in the left graph of figure 13, where the oscillations are small and smooth; it is the Fourier components of this smooth graph that are not smooth. The calculations are performed with the Algorithmic 'n Analytic Number Theory[7] multi-precision library (based on gnuMP); the results are verified by repeating the calculations at various different precisions.

## Counting the Zeros

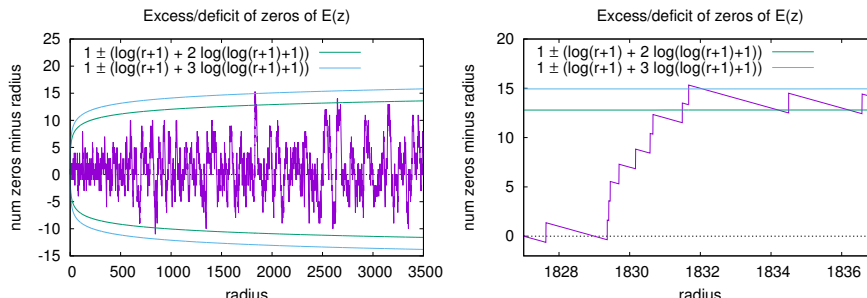
The zeros seem to be scattered very uniformly around the complex plane. How many are there? They are easy to count, using Cauchy's argument principle: one performs an integral of the phase around a circle of radius  $r$ ; this counts the number of zeros inside the circle. This counting is easy to perform numerically. The result is that there are almost exactly  $N$  zeros within radius  $N$  of the origin, the count being off by no more  $\mathcal{O}(\log(r))$ . The surplus or deficit of zeros, as a function of the enclosing radius, is shown in figure 15.

This figure suggests that the strict bound is  $1 \pm [\log(r+1) + M \log(\log(r+1) + 1)]$  with equality holding at  $r = 1$  (there is one zero inside of  $r = 1$ ). What's  $M$ ? Good question. If you only graphed out to  $r = 120$ , you might think that  $M = 1$  is a tight, but good bound. Not so, as it fails near  $r = 123$ . So maybe  $M = 2$ ? Sure, that works out to about  $r = 844$ , where it fails. So maybe  $M = 3$ ? Sure, that works out to about  $r = 1832$ , where it fails. So maybe  $M = 4$ ? Sure, why not, the figure supports that hypothesis.

Note that this linear dependence on the radius means that the density of zeros is decreasing as the square root — the area of a circle goes as  $r^2$ .

Proving this bound may be hard; similar bounds are known to be equivalent to the

Figure 15: Excess and Deficit of Zeros



The excess or deficit of zeros within a circle of a given radius. That is, the number of zeros within a circle of radius  $r$  is  $r$  plus the remainder shown above. The figure on the right is a close-up of what happens at  $r = 1832$ , where the count surpasses one of the hypothesized logarithmic bounds. Note that the data for these graphs was very compute-intensive to create: it represents several CPU-months of calculations.

Riemann hypothesis (examples include the bounds on Merten's conjecture (sums of the Möbius  $\mu$ ) and of Newton series expansions of the Riemann zeta (Flajolet's paper with me)[8], both of which have this characteristic square-root form). Of course, I have no clue if the zero-counting formula is equivalent to the Riemann hypothesis, but I would not be surprised.

## The Reciprocal

One may continue in this vein. Figure 16 shows the generating function for the reciprocal of the GPF function. To be precise, the figure shows the rescaled absolute value of

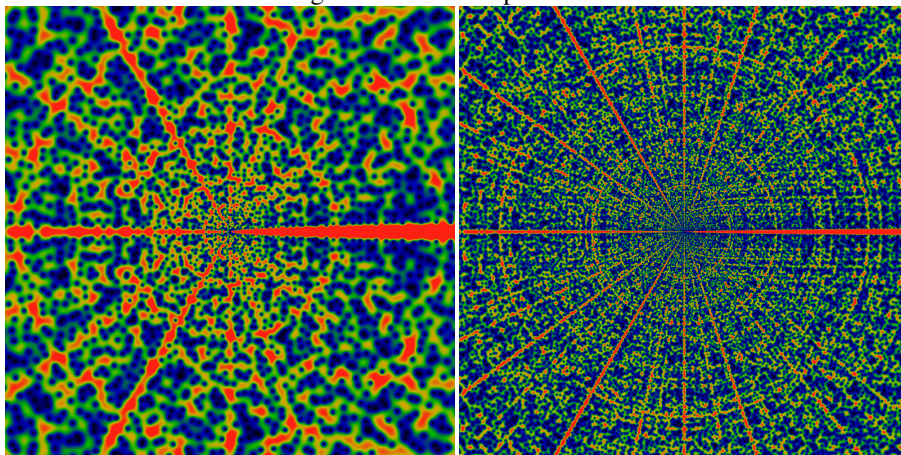
$$EG\left(\frac{1}{\text{gpf}}; z\right) = \sum_{n=1}^{\infty} \frac{1}{\text{gpf}(n)} \frac{z^n}{n!}$$

Clearly, there's a new feature visible here: rings! Concentric rings! Hard to tell, but, pulling out a ruler and eyeballing them, they seem to be located at powers of two: for the left image, the outermost ring is at a radius of 2048, then three more clearly visible ones are at 1024, 512 and 256. Hard to tell, but there is a vague hint of another ring at  $1536=3*512$ . And maybe yet many more rings! Wow! Who knew?

The right image in figure 16 shows something else now: visible lines paralleling the positive  $x$ -axis, seeming maybe to curl around the origin in some vaguely parabolic way. There's a particularly large pseudo-parabolic orbit visible, coming in from the right, about 3/4th's of the way up, turning around the origin, and exiting about 3/4th's of the way down (on the right, of course – its easy to see, once you see it.)

As before, there are hints of Moiré patterning along the  $x$ -axis, although this time, the scale of the picture is such that the individual zeros can still be distinctly made out.

Figure 16: The Reciprocal GPF



Both images show the exponential generating function for the reciprocal gpf, scaled to remove leading divergences. The left image shows the absolute value of

$$\frac{1}{3}e^{-|z|} \log^3 |z| EG\left(\frac{1}{\text{gpf}}; z\right)$$

on the domain  $-2160 \leq x, y \leq +2160$ . The color scale is as always: red corresponds to values of 1.0 or greater, while green is 0.5 and blue/black is 0.25 or less. The right image shows

$$0.005e^{-|z|} \log^5 |z| EG\left(\frac{1}{\text{gpf}}; z\right)$$

on the domain  $-2 \times 10^4 \leq x, y \leq +2 \times 10^4$ , with the same color scale. Clearly, the numerical estimation of the logarithmic terms in the asymptotic behavior is a bit ambiguous. In both cases, the asymptotic term was picked to give the appearance of a uniform color balance.

---

Therefore, the Moiré patterns cannot be *optical* pixel-scale effects – that is, its not an effect due to the finite size of the pixels – it does not meet the criteria for the classical, canonical definition of the Moiré effect in a computer graphics image. Instead, the Moiré patterning seems to actually exist within the function itself! This suggests that perhaps the function itself can be decomposed as a sum of "layers", each layer consisting of a very regular oscillatory pattern, with only the sum of the patterns resulting in the apparent chaos of the image.

What are all these features? How are they to be described? What do they correspond to? One can't help but get the sense that this is the projection of some structure on some bundle, some structure built of sheafs and germs, but quite how to get that is unclear.

What are these parabolic-like orbits? Well, there's an alternate plot that makes curve-fitting easier. The left image in figure 18 unwinds the the graph from around the origin, showing, much like the previous

$$1.6e^{-|z|} \log |z| \log^4 [\log (|z| + 1) + 1] EG \left( \frac{1}{\text{gpf}}; z \right)$$

except that here,  $z = re^{i\theta}$  with  $\theta$  running along the vertical axis, from 0 to  $\pi$ . Along the horizontal axis,  $r$  is plotted on a logarithmic scale, so that  $r$  runs from 1 on the left to 65536 on the right. Superimposed on this figure are five hand-fitted dashed white lines. One tries to capture the edge of the root-free zone. This line is given by  $\sin \theta/2 = 1/\sqrt{r}$ . Note the radical. Careful examination shows that at least a few zeros appear on the wrong side of this line – the shape seems to be only approximate. Four more curves try to fit the pseudo-parabolas. The fits are OK on the large- $r$  asymptotic region, but poor in the small- $r$  region. The four that are drawn are given by

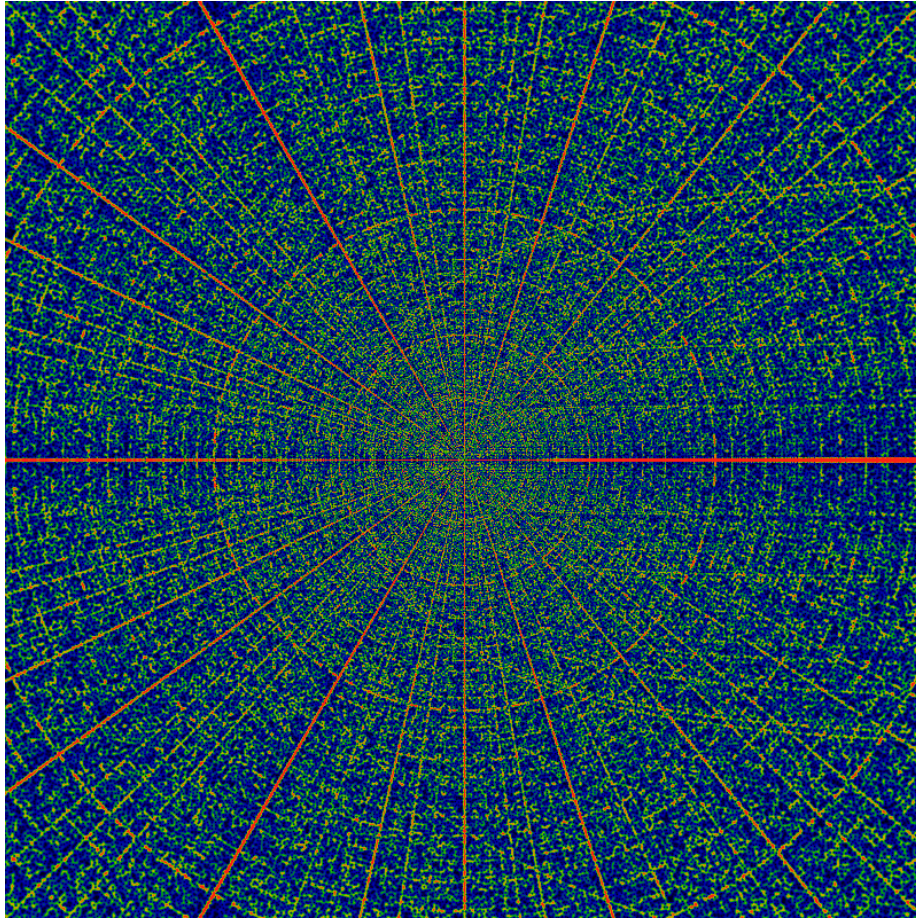
$$\frac{768}{r}, \frac{1200}{r}, \frac{1500}{r}, \frac{1948}{r} = \sin \frac{\theta}{2}$$

The integers in the above are approximate ... they are obtained by eyeballing. I tried to pick integers with a small number of prime factors, and these seem pretty close, but there is no obvious pattern that is emerging. It is worth spending a few minutes, looking at this under magnification.

What happened to the circles? This is a conformal map; they should be vertical lines! Well, they are still there, just too narrow to be visible in the left-most image. They do become visible, in the middle image: five evenly spaced vertical lines. The five vertical lines correspond to  $r = 2048, 4096, 8192, 16384, \text{ and } 32768$ , respectively. Otherwise, there is nothing particularly new in this image; everything visible here is visible in earlier images.

Just how thin are these vertical lines? The rightmost image is a closeup of the middle image in this case,  $r$  runs from  $(32768-650)$  to  $(32768+650)$ . Eye-balling the red strip, it seems maybe 350 units wide – so maybe a width of  $\sqrt{32768} = 362$  is a decent wild guess. Is this vertical stripe really zero-free? Hard to tell from this picture. There are lots of blue smears – there are about 650 zeros in this image (as demonstrated earlier, there are about  $r$  zeros inside a circle of radius  $r$ ; the width of this image is  $650+650$  but the height is only  $\pi$  and not  $2\pi$ .) Fiddling with the color-map

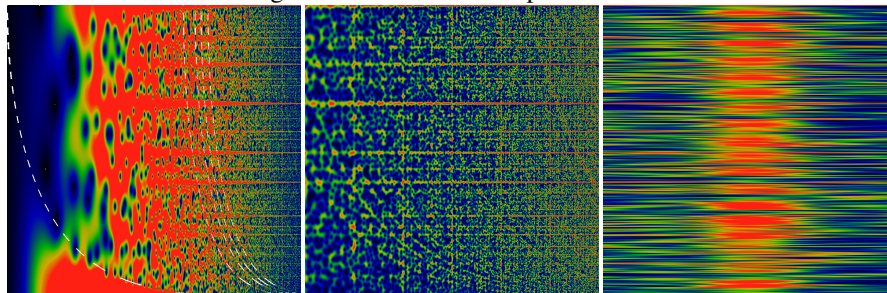
Figure 17: Zoomed Reciprocal GPF



Just as the previous figure, this shows the exponential generating function for the reciprocal gpf, but for a wider domain  $-1.2 \times 10^5 \leq x, y \leq +1.2 \times 10^5$ . Note that there are parabola-like orbits facing to the left and to the right. Those aimed to the right are obviously visible; those to the left are extremely faint. There are also hints of other trceries, but its hard to say if these are merely optical, visual field effects or if they have some basis in mathematical reality. The prominent parabola-like orbits appear to be described by the curve  $C = r \sin \theta/2$  for constants  $C$ .

---

Figure 18: Unwound Reciprocal GPF



All images use a mapping  $z = re^{i\theta}$  with  $r$  running along the horizontal axis, left to right, and  $\theta$  along the vertical axis, from  $\theta = 0$  at the bottom, and  $\theta = \pi$  at the top. The horizontal scale is logarithmic. The left image shows  $1 \leq r \leq 65536$ , the middle image has  $1024 \leq r \leq 65536$ , and the right image shows the much tighter range  $32768 - 650 \leq r \leq 32768 + 650$ . The dashed white lines in the left figure are attempts to guess at locations of curves; they are as explained in the text.

---

helps isolate some of these a bit more clearly, and it seems like there might be dozen or two zeros actually within the red stripe, rather than all the blue being just a smear from outside the stripe.

Why are there parabolas? Because, one might say, we are plotting the function wrong. The parabola-like curves are given by  $C = r \sin \theta / 2$  for constants  $C$ . But this curve is just what the straight line  $C = r \sin \theta$  would look like under a conformal map  $z \rightarrow z^2$ . This suggests that perhaps a more natural setting is the Poincaré upper-half-plane; that is, the complex upper-half-plane endowed with the Poincaré metric. With this setting, the radial lines become vertical lines; the circles become horizontal lines, and the pseudo-parabolas become half-circles, terminating on the  $y = 0$  horizon. Presumably, this can make a modular symmetry apparent.

## The Reciprocal Squared

The figure 19 shows

$$EG\left(\frac{1}{\text{gpf}^2}; z\right) = \sum_{n=1}^{\infty} \frac{1}{\text{gpf}^2(n)} \frac{z^n}{n!}$$

with the domain  $-2160 \leq x, y \leq 2160$ . As usual, the leading order of  $\exp |z|$  has been removed. The circular rings are far more prominent, now. The primary sequence seems to be located at powers of 2; so that, here, the outermost ring appears to be of radius 2048; the middle one presumably with a radius of 1024, etc. The other rings are presumably at other powers of various different primes.

Figure 19: Reciprocal Squared

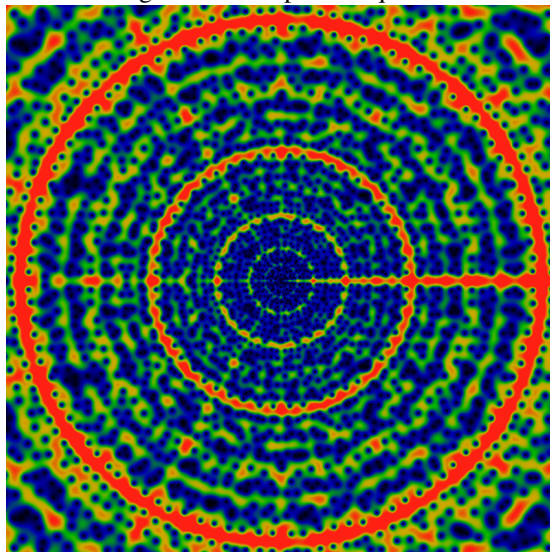
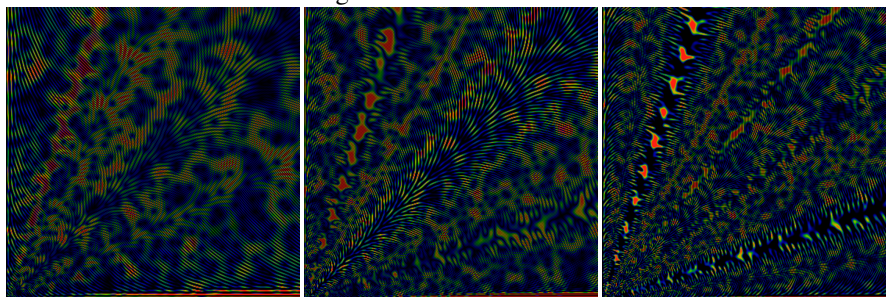


Figure 20: Moiré Patterns

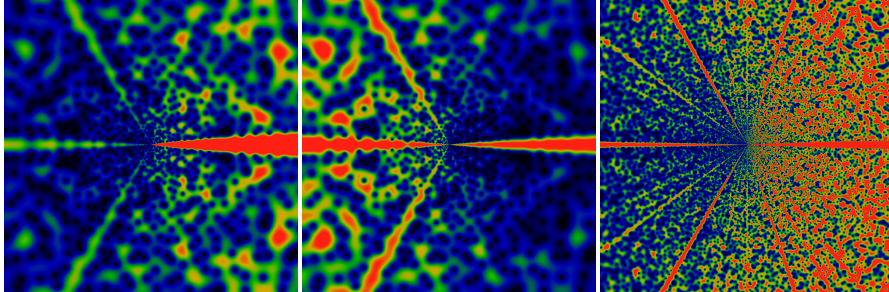


## Moiré Patterns

Figure 20 show actual Moiré patterns! All three images show the real part of  $EG(\text{gpf}; z) e^{-|z|}$ . As noted at the very beginning, the phase portrait in figure 2, the phase forms radially oriented fingers. Likewise, the real part of the function consists of radially oriented, roughly sinusoidal ridges and valleys. At the scale of this image, the distance between peak and trough is less than one pixel, and so by using a sharp sampling, one necessarily gets a sampling aliasing effect (spatial Nyquist aliasing). The left image is 400x400 pixels in size, and it shows a region  $0 \leq x, y \leq 2000$  (the upper-right quadrant). The Moiré patterning gives a hint about how the radial fingers differ from being perfectly radial.

The middle image shows the region  $0 \leq x, y \leq 4000$ . Of course, Moiré patterning is very sensitive to the sampling frequency. The rightmost image shows  $0 \leq x, y \leq 8000$ .

Figure 21: Pochhammer Generating Functions



## The Pochhammer Symbol

One last diversion. The left image of figure 21 shows the greatest prime factor, using the rising Pochhammer symbol in the generating function. Its normalized by a factorial, for convergence, so it perhaps should be called a binomial coefficient generating function. Specifically, define

$$\text{RPG}(f; z) = \sum_{n=1}^{\infty} f(n) \frac{(z)_n}{(n!)^2}$$

where  $(z)_n = z(z+1)(z+2)\cdots(z+n-1)$  is the rising Pochhammer symbol. The two factorials in the denominator guarantee convergence, as otherwise the sum is badly behaved. The leading divergence is removed; the graph shows  $\text{RPG}(\text{gpf}; z) \exp(-2\sqrt{|z|})/|z|$ .

Notice the  $\sqrt{|z|}$  in the normalization: such binomial-coefficient sums (Newton series, if given their proper name) are "well-known" to diverge in this kind of square-root fashion.[8] As before, there seem to be zero-free rays at angles  $\theta = 0$  and  $\pi$ ; of course, and at  $2\pi/3$  and, harder to discern, at  $2\pi/5$ . Presumably all the other rationals are there too; they are not very clear in this picture. The domain in this picture is just huge:  $-10^6 \leq x, y \leq 10^6$  – this is far far wider than any of the previous images: the zeros are much, much farther apart.

One may also consider a very similar sum, using the falling Pochhammer symbol, instead of the rising one. This symbol is given by  $z^{(n)} = z(z-1)(z-2)\cdots(z-n+1)$ . The resulting image appears below, it is of  $\text{FPG}(\text{gpf}; z) \exp(-2\sqrt{|z|})/|z|$ . The scale is again  $-10^6 \leq x, y \leq 10^6$ .

Some of the first few zeros for the rising Pochhammer generating function are shown below. Note that the first two lie precisely on the real axis. The others do not seem to occur at any low rational angle (the column  $\varphi$  shows the angle in units of  $\pi$ , thus a value of  $\varphi$  of one indicates the negative  $x$ -axis), although the next few seem to try to get close to the 3rd roots of unity, and the one after that the 6th root of unity. After that, there is no clear progression. As before, they are presumably transcendental, rather than, for example, quadratic irrationals, or some such.

$r$	$\varphi$	$x$	$y$
1.3949092398684	1	-1.3949092398684	0
4.5626759564288	1	-4.5626759564288	0
10.245898379007	0.64420879547681	-4.4846874842696	9.2122750589292
24.83352515618	0.63379620727208	-10.133683877231	22.671842068058
55.576607747775	0.3205855915997	29.693058011758	46.979587425396
72.25879634152	0.8121672651601	-60.038996469216	40.207618080342
117.75420722502	0.46759200907347	11.968172804434	117.1444243612
192.15199916793	0.81693429156798	-161.24015864602	104.51795072638
201.03591391007	0.25107689390384	141.67211584758	142.63397306717
285.6352301736	0.54737231184267	-42.35277394865	282.47783498034
364.85530526812	0.27307016022456	238.63224457153	275.99645945745
442.19734166307	0.78730029361836	-347.09323384104	273.97951747467

The table below shows the first few zeros for the falling Pochhammer generating function. Note that the zeros differ from those above. Note that they all seem to be close to, but not quite on, 4th and 8th and 16th roots of unity.

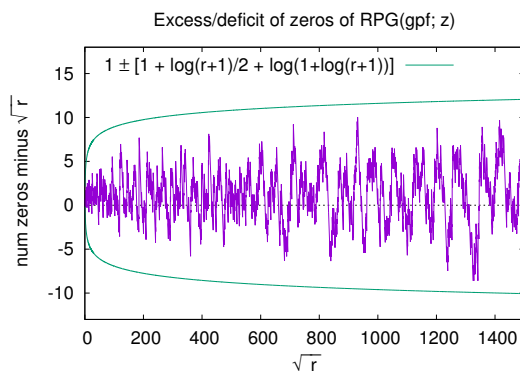
$r$	$\varphi$	$x$	$y$
0.72183600549901	0.49137876622082	0.019548108331473	0.72157126487647
10.360150450484	0.45106261529342	1.5865160932827	10.237953117808
23.302941560009	0.47588077521583	1.7640394756877	23.236076477697
57.987569085342	0.7605584350114	-42.340693875438	39.621002139948
67.48077369795	0.26157732931857	45.949442919987	49.419667281528
122.32995335662	0.40689342952179	35.273809336995	117.13400814063
168.26853286447	0.78918215559082	-132.69280305254	103.4742439954
224.60980862841	0.22477866727782	170.89602763141	145.75360672003
281.86194385292	0.50767619198356	-6.7965739748906	281.77998859881
393.67913951173	0.2492135681373	279.06010117129	277.68457793146
410.84081343407	0.76652914265676	-305.19542443344	275.03804625552

The right-most image is for the rising Pochhammer generating function, but showing the domain  $-1.6 \times 10^8 \leq x, y \leq 1.6 \times 10^8$  – again, this is several orders of magnitude wider than any earlier graphics.

Although superficially similar to the other graphs shown previously, this is different. Note that the zeros far from the origin are clearly distinguishable visually, unlike those near the origin: this indicates that the density of zeros is falling like the square of the radius, that is, as the area of the graphic. This is already suggested by the divergence of the function going as exp of the square-root of the radius – as if the density of zeros is tied to the rate of divergence of the function along some radial ray.

How many zeros are there? As before, we have the curious similarity: the bound on the rate of divergence of the function gives the count of the zeros. Thus, asymptotically

Figure 22: Excess/Deficit of zeros of RPG (gpf; z)



RPG (gpf; z) seems to go roughly as  $\mathcal{O}\left(|z| e^{2\sqrt{|z|}}\right)$ . The number of zeros inside a circle of radius  $|z|$  appears to be given by  $1 + \sqrt{|z|}$  and the error of this approximation is bounded by

$$\pm \left[ 1 + \frac{1}{2} \log(1 + |z|) + \log(1 + \log(1 + |z|)) \right]$$

as shown in figure 22. This bound appears to be tight; nothing tighter seems to work. Note that this bound extends all the way to  $|z| = 0$  – that is, it is not violated at small  $|z|$ .

## Conclusion

The use of exponential generating functions with almost any classical arithmetic function arising in number theory (such as the divisor function, the Euler totient, the prime counting function, *etc.*) is very nearly unheard of, and tackling the greatest prime factor in this way is unique. Why would that be so? Because there are no known results for the exponential generating function in this setting. This is in sharp contrast to the Dirichlet generating function (i.e. the Dirichlet series) or the Lambert generating function (Lambert series) which have a vast number of identities commonly presented in undergraduate number theory courses.[9]

The visually apparent symmetries in the images here makes it quite clear that there is some sort of distorted modular symmetry at work, apparent just out of easy reach. The figures here whet the appetite. Perhaps a proper theory of these figures would start with something simpler than the greatest prime factor function: certainly the divisor function and the Euler totient function appear to be far more regularly patterned, when passed through the exponential generating function. But even then, although there is a tremendous visual regularity to those figures, it still seems impossible to obtain closed form solutions. So the best one can do for now is to stare in wonder.

## References

- [1] Eric W. Weisstein, “Greatest Prime Factor”, , 2016, URL <http://mathworld.wolfram.com/GreatestPrimeFactor.html>, from MathWorld—A Wolfram Web Resource.
- [2] N. J. A. Sloane, “Greatest Prime Factor”, , 2016, URL <http://oeis.org/A006530>, online Encyclopedia of Integer Sequences.
- [3] Linas Vepstas, “The Minkowski Question Mark,  $PSL(2,Z)$  and the Modular Group”, , 2004, URL <https://www.linas.org/math/chap-minkowski.pdf>, self-published on personal website.
- [4] Linas Vepstas, “On the Minkowski Measure”, *ArXiv*, arXiv:0810.1265, 2008, URL <http://arxiv.org/abs/0810.1265>.
- [5] Linas Vepstas, “The Number Theory Room”, , 2005, URL <https://www.linas.org/art-gallery/numberetic/numberetic.html>, from Linas Vepstas’ Art Gallery.
- [6] Simon Plouffe, “Plouffe’s Inverter”, , 1995, <http://pi.lacim.uqam.ca/>.
- [7] Linas Vepstas, “Algorithmic ’n Analytic Number Theory Multi-Precision Library”, , 2004, URL <https://github.com/linas/anant>.
- [8] Philippe Flajolet and Linas Vepstas, “On Differences of Zeta Values”, *Journal of Computational and Applied Mathematics*, 220, 2007, pp. 58–73, URL <http://arxiv.org/abs/math/0611332v2>, arxiv:math.CA/0611332v2.
- [9] Tom M. Apostol, *Introduction to Analytic Number Theory*, Springer; New York, 1976.